HIGH *Q* LOW INPEDANCE WLCSP RESONATOR FOR SUB-100 MHZ PROGRAMMABLE OSCILLATOR APPLICATION

Guoqiang Wu[1], Jinghui Xu[1], Xiaolin Zhang[1], Nan Wang[1], Danlei Yan[1], Jayce Lay Keng Lim[1], Yao Zhu[1], Wei Li[2], and Yuandong Gu[1]

[1]Institute of Microelectronics, Agency for Science, Technology and Research (A*STAR), Singapore
[2]Exploit Technologies Pte Ltd (ETPL), Agency for Science, Technology and Research (A*STAR), Singapore

ABSTRACT

A high performance aluminum nitride (AlN) on silicon piezoelectric resonator is reported in this paper. The resonator is fabricated based on the AlN on cavity-silicon-on-insulator (SOI) platform and vacuum encapsulated using the wafer level chip scale packaging (WLCSP) via aluminum-germanium (Al-Ge) eutectic bonding approach. After dicing, the resonator has an attractive compact size of 0.6×0.6×0.7 mm^3. The fabricated resonator achieves a quality factor (Q) of 9517 and an impedance of 51 Ohm at its resonant frequency of 27.19 MHz. The measured frequency drift is within 30 ppm after 1000 thermal cycles (-45 °C to 85 °C). No obvious impedance change caused by the thermal cycles is observed. The piezoelectric resonator based programmable oscillator shows an overall frequency drift of 3 ppm over the temperature range of -20 °C to 70 °C, thanks to the passive and active temperature compensation approaches. With this stable frequency reference, the programmable oscillator produces a 76.4 MHz frequency output with an integrated phase jitter of 2.21ps from 12 kHz to 10 MHz.

INTRODUCTION

Recently, micro-electro-mechanical systems (MEMS) resonators have gained much attention due to their small size, good performance and high compatibility with the standard complementary-metal–oxide–semiconductor (CMOS) process [1-5]. Although the quartz crystal resonators have served the electronics industry very well for almost 100 years and they are still dominating the whole timing market, they suffer from several disadvantages compared with the MEMS resonators [6, 7]. The major advantage of MEMS resonators over quartz crystal resonators is the integration with the CMOS circuits [1-7]. Secondly, MEMS resonators are more immune to external environmental noises, such as vibration, shock and electromagnetic interference (EMI) than quartz resonators. Moreover, the MEMS resonators can be easily batch manufactured and packaged, which results in lower cost.

There are two dominating technologies for the MEMS based resonators [1, 2]. One is based on the electrostatic approach and the other is using the piezoelectric approach. The electrostatic resonators usually employ the single crystal silicon (SCS) or polycrystalline silicon as the structure material and demonstrate attractive quality factors (Qs) as high as few millions [8, 9]. However, the electrostatic resonators suffer from high motional impedance and very low electro-mechanical transduction efficiency. In order to reduce the motional impedance, a large DC bias and very narrow capacitive transducer gaps as small as few hundred nanometers are required. Large DC voltage may cause additional nonlinearity to the resonators and the narrow gaps require very precise process control, which increase the complexity of the fabrication process [10, 11]. The piezoelectric resonators have higher electro-mechanical coupling coefficiency, which results in a lower motional impedance. While the piezoelectric resonators have a relative lower Q compared with the capacitive resonators. No narrow gaps are required, making the piezoelectric resonators easy to achieve batch manufacture with good process uniformity.

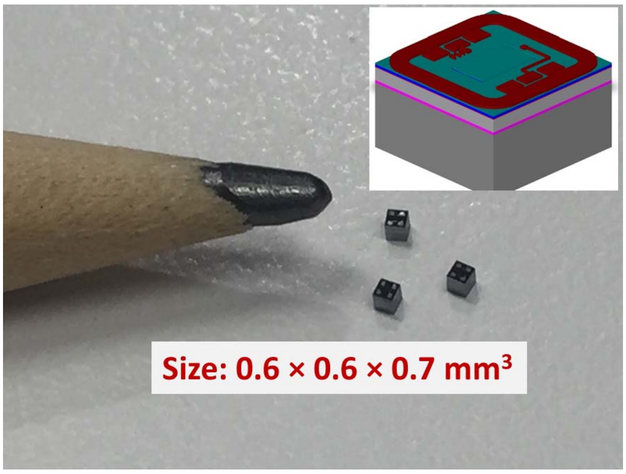

Figure 1: Optical image of the diced WLSCP piezoelectric resonators. The inset shows the three dimensional model of the resonator before packaging.

In order to take both the advantages of high Q from the SCS electrostatic resonators and high electromechanical coupling coefficiency from the piezoelectric resonators, thin-film piezoelectric on silicon resonators are developed [12]. In this paper, we report a wafer level chip scale packaged (WLCSP) aluminum nitride (AlN) on cavity-SOI piezoelectric resonator, which shows both high Q and low impedance. The fabricated AlN on cavity-SOI piezoelectric resonator features an attractive small size of 0.6×0.6×0.7 mm^3 after dicing, as shown in Figure 1.

ALN ON CAVITY-SOI PLATFORM

The reported AlN piezoelectric resonators are fabricated based on a cavity-SOI platform and vacuum encapsulated using the WLCSP approaches. Figure 2 illustrates the cross sectional view of the reported piezoelectric resonators in our work.

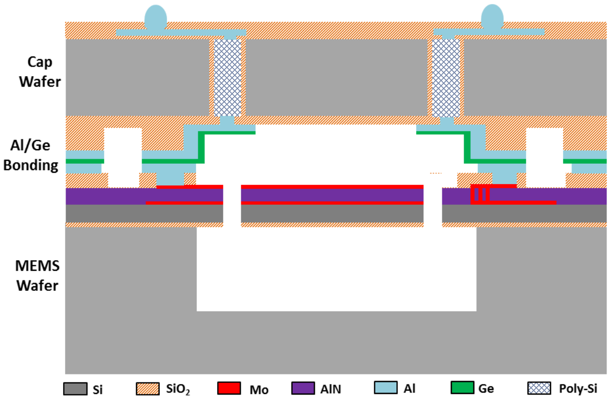

Figure 2: Cross sectional view of the demonstrated WLCSP piezoelectric resonator. The AlN on silicon piezoelectric MEMS resonator is fabricated based on a cavity-SOI wafer. A cap wafer with poly-silicon through silicon vias (TSVs) is bonded with the device wafer to achieve a vacuum encapsulation using the Al-Ge eutectic bonding approach.

The fabrication process starts with an 8 inch customized cavity-SOI wafer with 5-µm-thick device layer. The buried oxide layer underneath the silicon structure layer also serves as a passive temperature compensation layer, which is used to minimize the temperature coefficient of frequency (TCF) of the resonator [13, 14]. Then the Mo-AlN-Mo sandwiched layers are deposited on top of the silicon structure to form the piezoelectric actuation layers. Following the deposition and patterning of an aluminum layer to form the bonding pads as well as the sealing ring, the device structures are patterned and achieved by etching the Mo-AlN-Mo-Si stack layers one after the other. After that, a cap wafer with poly-silicon through silicon vias (TSVs) is bonded with the device wafer to achieve a vacuum encapsulation using the Al-Ge eutectic bonding approach.

The Al-Ge vacuum WLCSP approach not only protects the MEMS resonators from the external mechanical damage, but also achieves a better performance by eliminating the air damping of the resonators. Moreover, it largely shrinks the size of the MEMS resonators.

MEASUREMENT RESULTS

The fabricated piezoelectric resonators are measured with a Keysight impedance analyzer E4490A. Before the measurement, the standard phase compensation and open-short-load calibrations are implemented. The measured impedance curve of a fabricated piezoelectric resonator is shown in Figure 3. A Q of 9517 and an impedance of 51 Ohm at its resonant frequency of 27.19 MHz are directly obtained from the measurement. Both high Q and low impedance are achieved thanks to the advanced AlN on silicon architecture. A perfect phase change of around 175 degree is achieved.

In order to verify the reliability and robust of the vacuum bonding quality, a 1000 thermal cycles (-45 °C ~ 85 °C) are implemented to verify the long term stability of the packaged piezoelectric resonators. The long stability is a key parameter for resonators to achieve high accurate frequency reference over its life time. After 100, 300, 500, 800, and 1000 thermal cycles, the piezoelectric resonators are tested at the room temperature to obtain their impedance responses.

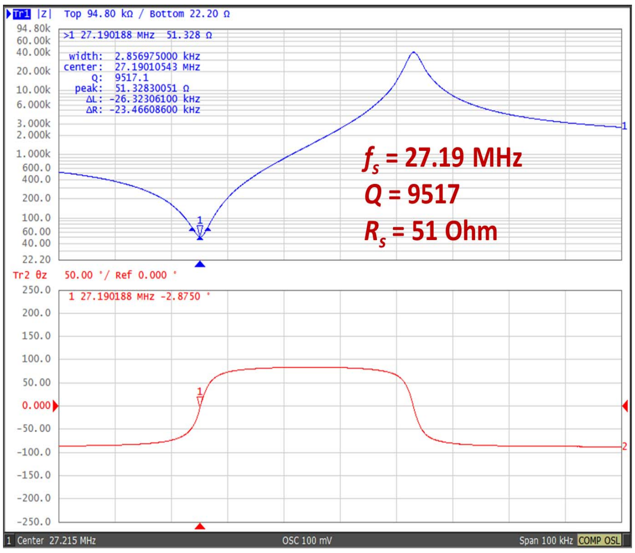

Figure 3: Measured impedance curves of the piezoelectric resonator: magnitude (upper) and phase (lower). The measured Q is 9517 and the impedance is 51 ohm.

Figure 4 shows the measured series resonant frequencies (f_s) and impedance drifts of four resonators in thermal cycles. The frequency drifts are less than 30 ppm and the impedance drifts are within 10%. The low drifts of the frequency and impedance indicate the robust fabrication process and good long term stability of the resonators.

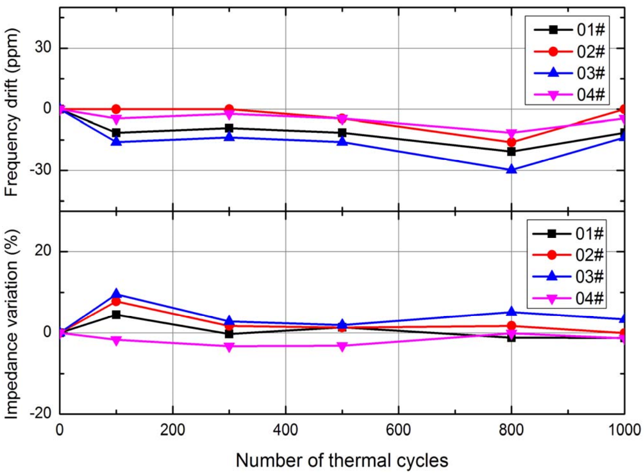

Figure 4: Measured frequencies and impedance drifts of the piezoelectric resonators within 1000 thermal cycles from -45 °C to 85 °C. The measurements are done at room temperature.

OSCILLATOR PERFORMANCE

The diced MEMS piezoelectric resonator is interfaced with a customized application specific integrated circuit (ASIC) to achieve a programmable oscillator. Figure 5 shows the block diagram of the programmable oscillator. A temperature sensor and a digital compensation engine are employed to implement the active temperature compensation using a third order polynomial correction. The fractional-N phase locked loop (PLL) is used to output a stable frequency output over the full temperature range. A programmable counter form 1 MHz to 100MHz output frequency is achieved with the reference frequency from the MEMS resonators.

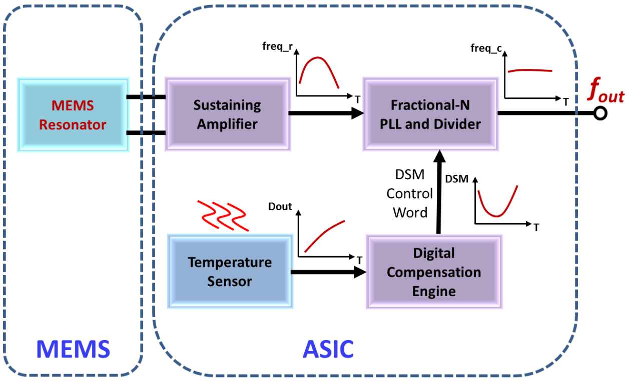

Figure 5: The block diagram of ASIC for the piezoelectric resonator. A temperature sensor and a digital compensation engine are employed to implement the active temperature compensation using a third order polynomial correction.

The dependence of the output frequency on operating temperature of the piezoelectric resonator based oscillator is recorded to obtain its temperature characteristics. Figure 6 shows the measured output frequency drifts of the oscillator before and after the active temperature compensation in the temperature range of -20 °C to 70 °C. Without the active compensation, the frequency drift is less than 160 ppm in the full temperature range thanks to the passive compensation of the buried oxide layer underneath the silicon structure. The passive compensation approach is based on the addition of a material with positive temperature coefficient of Young's modulus (TCE), such as SiO_2, stacking on the silicon structure layer to create a composite resonator with reduced overall TCF [13-15].

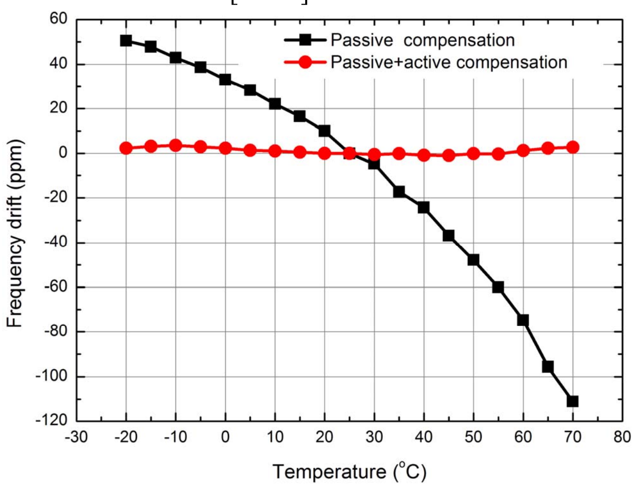

Figure 6: Comparison of the measured output frequency drifts of the MEMS oscillator before and after the active temperature compensations in the temperature range of -20 °C to 70 °C.

Active temperature compensation is also implemented in this work [16, 17] in order to further reduce the temperature drift over the environmental temperature. A temperature sensor embedded in the ASIC is used to detect the chip temperature. A digital compensation engine provides a proper control word for the fractional-N synthesizer using the third-order polynomial correction. After the active compensation, the frequency drift is further reduced to 3 ppm in the temperature range of -20 °C to 70 °C.

With the MEMS resonator as a stable frequency reference, the programmable oscillator with 1 MHz to 100 MHz frequency output is achieved. Figure 7 shows the measured phase noise of the PLL output at 76.4 MHz. The measured phase noises are -108 dBc/Hz, -123 dBc/Hz and -136 dBc/Hz with offsets of 12 kHz, 100 kHz and 1 MHz, respectively. The RMS integrated phase jitter is 2.21 ps from 12 kHz to 10 MHz.

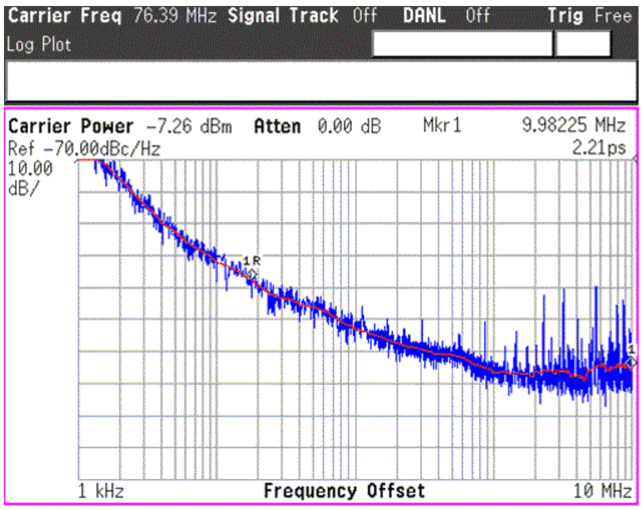

Figure 7: Measured phase noise of the PLL frequency output at 76.4 MHz with the 27.19 MHz piezoelectric oscillator as the frequency reference. The RMS integrated phase jitter is 2.21 ps from 12 kHz to 10 MHz.

This paper reports a WLCSP MEMS piezoelectric resonator using the Al-Ge eutectic bonding approach. The fabricated piezoelectric resonator features a compact size and shows a high performance. Thermal cycling testing is implemented to evaluate the long term stability of the MEMS resonator. With this stable frequency reference, a programmable oscillator with 1 MHz to 100 MHz frequency output is achieved with low phase noise.

ACKNOWLEDGEMENTS

This work was partially supported by ETPL_14-R15GAP-0012_MEMS Timing Device. This study is also part of technology commercialization project, MEMSing, supported by Exploit Technologies Pte Ltd, A*STAR. The team helps companies to capture the opportunities in Internet of Things (IoT) market through our MEMS sensor/actuator portfolio and technology service.

REFERENCES

[1] C. T.-C. Nguyen, "MEMS technology for timing and frequency control", *IEEE Trans. Ultrason. Ferroelectr. Freq. Control,* vol. 54, no. 2, pp. 251–270, 2007.

[2] J. T. M. van Beek and R. Puers, "A review of MEMS oscillators for frequency reference and timing applications," *J. Micromech. Microeng.*, vol. 22, no. 1, p. 013001, 2012.

[3] R. N. Candler, M. A. Hopcroft, B. Kim, W. T. Park, R. Melamud, M. Agarwal, G. Yama, A. Partridge, M. Lutz, and T. W. Kenny, "Long term and accelerated life testing of a novel single-wafer vacuum encapsulation for MEMS resonators," *J. Microelectromech. Syst.*, vol. 15, no. 6, pp. 1446–1456, 2006.

[4] G. Q. Wu, D. H. Xu, B. Xiong, and Y. L. Wang, "A high-performance bulk mode single crystal silicon microresonator based on a cavity-SOI wafer", *J. Micromech. Microeng.*, vol. 22, no. 2, p. 025020, 2012.

[5] G. Q. Wu, D. H. Xu, B. Xiong, Y. C. Wang, Y. L. Wang, and Y. L. Ma, "Wafer-Level Vacuum Packaging for MEMS Resonators Using Glass Frit Bonding," *J. Microelectromech. Syst.*, vol. 21, no. 6, pp. 1484-1491, 2012.

[6] C. S. Lam, "A review of the recent development of MEMS and crystal oscillators and their impacts on the frequency control products industry", in *Proc. IEEE International Ultrasonics Symposium*, Beijing, China, November 2-5, 2008, pp. 694-704.

[7] K. J. Schoepf, R. Rebel, D. M. Chen, G. Zolfagharkhani, A. Gaidarzhy, J. H. Kuypers, M. Crowley, and P. Mohanty, "TCMO™: A Versatile MEMS Oscillator Timing Platform", In *Proc. Precise Time and Time Interval (PTTI) Meeting*, Santa Ana Pueblo, New Mexico, November 16-19, 2009, pp. 481-492.

[8] J. E. Y. Lee, J. Yan, and A. A. Seshia, "Low loss HF band SOI wine glass bulk mode capacitive square-plate resonator", *J. Micromech. Microeng.*, vol. 19, no. 7, p. 074003, 2009.

[9] G. Q. Wu, D. H. Xu, B. Xiong, and Y. L. Wang, "High Q Single Crystal Silicon Micromechanical Resonators With Hybrid Etching Process", *IEEE Sensors J.*, vol. 12, no. 7, pp. 2414-2415, 2012.

[10] L. Khine and M. Palaniapan, "High-Q bulk-mode SOI square resonators with straight-beam anchors", *J. Micromech. Microeng.*, vol. 19, no. 1, p. 015017, 2009.

[11] T. J. Cheng and S. A. Bhave, "High-Q, low impedance polysilicon resonators with 10 nm air gaps," in *Proc. 23rd IEEE Int. Micro Electro. Mech. Syst. (MEMS) Conf.*, Cancun, Mexico, January 24-28, 2010, pp. 695–698.

[12] A. Jaakkola, P. Rosenberg, S. Asmala, A. Nurmela, T. Pensala, T. Riekkinen, J. Dekker, T. Mattila, A. Alastalo, O. Holmgren, K. Kokkonen, "Piezoelectrically transduced single-crystal-silicon plate resonators", in *Proc. IEEE Ultrason. Symp.*, pp. 717-720, Beijing, China, November 2-5, 2008.

[13] A. K. Samarao, G. Casinovi, and F. Ayazi, "Passive TCF compensation in high Q silicon micromechanical resonators", in *Proc. 23rd IEEE Int. Micro Electro. Mech. Syst. (MEMS) Conf.*, Cancun, Mexico, January 24-28, 2010, pp. 116–119.

[14] R. Melamud, S. A. Chandorkar, B. Kim, H. K. Lee, J. C. Salvia, G. Bahl, M. A. Hopcroft, and T. W. Kenny, "Temperature insensitive composite micromechanical resonators", *J. Microelectromech. Syst.*, vol. 18, no. 6, pp. 1409–1419, 2009.

[15] N. Wang, J. H. Xu, X. L. Zhang, G. Q. Wu, Y. Zhu, W. Li, and Y. D. Gu, "Methods for precisely controlling the residual stress and temperature coefficient of the frequency of a MEMS resonator based on an AlN cavity silicon-on-insulator platform", *J. Micromech. Microeng.*, vol. 26, no. 7, p. 074003, 2016.

[16] M. H. Perrott, J. C. Salvia; F. S. Lee, A. Partridge, S. Mukherjee, C. Arft, J. Kim, N. Arumugam, P. Gupta, S. Tabatabaei, S. Pamarti, H. Lee, and F. Assaderaghi, "A temperature-to-digital converter for a MEMS-based programmable oscillator with <0.5-ppm frequency Stability and <1-ps Integrated Jitter", *J. Solid-State Circuits*, vol. 48, no. 1, pp. 276-291, 2013.

[17] A. Baschirotto, K. A.A. Makinwa, and P. Harpe, *Frequency references, power management for SoC, and smart wireless interfaces*. Springer, 2013.

CONTACT

*Jinghui Xu, tel: +65-67705663, xuj@ime.a-star.edu.sg;

Yuandong Gu, tel: +65-67705915, guyd@ime.a-star.edu.sg.